

Effects of Vehicle Speed and Engine Load on Motor Vehicle Emissions

ANDREW J. KEAN,[†]
ROBERT A. HARLEY,^{*,‡} AND
GARY R. KENDALL[§]

Department of Mechanical Engineering, University of California, Berkeley, California 94720-1740, Department of Civil and Environmental Engineering, University of California, Berkeley, California 94720-1710, and Technical Services Division, Bay Area Air Quality Management District, 939 Ellis Street, San Francisco, California 94109

Laboratory studies have provided a foundation of knowledge regarding vehicle emissions, but questions remain regarding the relationship between on-road vehicle emissions and changes in vehicle speed and engine load that occur as driving conditions change. Light-duty vehicle emissions of CO, NO_x, and NMHC were quantified as functions of vehicle speed and engine load in a California highway tunnel for downhill and uphill traffic on a ~4% grade. Emissions were measured throughout the day; average speed decreased inside the tunnel as traffic volume increased. Emissions of CO were typically 16–34 g L⁻¹ (i.e., grams of CO emitted per liter of gasoline consumed) during downhill driving and ranged from 27 to 75 g L⁻¹ during uphill driving. Downhill driving and moderate-speed uphill driving resulted in similar CO emission factors. The factor of 2 increase in CO emissions observed during higher-speed uphill driving is likely evidence of enriched engine fuel/air ratios; this was unexpected because uphill driving observed in this study occurred at moderate engine loads within the range experienced during the city driving cycle of the U.S. emissions certification test. Emissions of NO_x (as NO₂) were typically 1.1–3.3 g L⁻¹ for downhill driving and varied between 3.8 and 5.3 g L⁻¹ for uphill driving. Unlike observations for CO, all uphill driving conditions resulted in higher NO_x emission factors as compared to downhill driving. NO_x emissions increased with vehicle speed for uphill driving but not as strongly as CO emissions. Emissions of CO and NO_x are functions of both vehicle speed and specific power; neither parameter alone captures all the relevant effects on emissions. In contrast to results for CO and NO_x reported here and results for NMHC reported previously by Pierson et al. (*Atmos. Environ.* **1996**, *30*, 2233–2256), emissions of NMHC per unit of fuel burned for downhill driving were over 3 times greater than NMHC emissions for uphill driving. Emission rates of CO and NO_x varied more with driving conditions when expressed per unit distance traveled rather than per unit fuel burned while NMHC

emission rates normalized to distance traveled were approximately constant for uphill versus downhill driving during peak traffic periods.

Introduction

Motor vehicles are an important source of carbon dioxide, carbon monoxide, volatile organic compounds, nitrogen oxides, and particulate matter (1). A key gap in our understanding of these emissions is the effect of changes in vehicle speed and engine load on average emission rates for the on-road vehicle fleet. Engine load and vehicle speed are closely linked to fuel consumption and pollutant emission rates. Factors that affect engine load directly include wind resistance, tire–roadway friction, vehicle acceleration, roadway grade, engine friction, and use of accessories such as air conditioning. These sources of engine load are in turn determined by a combination of vehicle attributes (e.g., engine displacement, vehicle mass, transmission efficiency) and vehicle operating conditions. Operating conditions such as vehicle speed and acceleration are affected by traffic congestion, driver mentality, traffic signals, posted speed limits, etc. Improved understanding of the link between operating conditions and emissions will help in the assessment of interventions such as adding lanes to highways, traffic signal synchronization, traffic calming measures, on-ramp metering, and changing/enforcing posted speed limits.

Under high-load conditions, some engines are mandated to operate fuel-rich (2–6). This maximizes engine torque, reduces knock, and protects the catalytic converter from excessive temperatures. While operating fuel-rich, emissions of CO and VOC increase dramatically. Remote sensing studies also show that exhaust HC concentrations are high under coasting or braking conditions (7), although fuel throughput is low under light-load operating conditions.

Progress has been made in developing modal emissions models (8–12), most of which use results of laboratory testing of individual vehicles. However, it has proved costly and difficult to acquire a large enough random sample of in-use vehicles to ensure that the overwhelming contribution to total fleet emissions by malfunctioning/high-emitting vehicles is represented accurately. Also, high-emitting vehicles often behave erratically in the limited laboratory testing that has been done (13). On-road measurements provide a complementary approach to studying vehicle emissions and are needed to provide field data against which to evaluate predictions of modal emissions models (14).

Roadway tunnels enable measurement of emissions from large numbers of on-road vehicles (15–22). These investigations take advantage of the fact that emissions from motor vehicles inside tunnels can be isolated from other sources. Unlike remote sensing, which measures emissions of individual vehicles as they drive by a roadside sensor, tunnel studies provide fleet-average emission results. A previous tunnel study that addressed the effect of roadway grade and, consequently, engine load on exhaust emissions was performed by Pierson et al. (16). That study found that driving uphill on a 3.8% grade roughly doubled CO and NO_x emission factors expressed per unit distance traveled and increased the VOC emission factor by 50% as compared to downhill driving on a 0.6–3.8% grade in the Fort McHenry Tunnel. When normalized to fuel consumed rather than distance traveled, emission rates of CO, VOC, and NO_x for uphill and downhill driving were all the same within experimental

* Corresponding author phone: (510)643-9168; fax: (510)642-7483; e-mail: harley@ce.berkeley.edu.

[†] Department of Mechanical Engineering, University of California.

[‡] Department of Civil and Environmental Engineering, University of California.

[§] Technical Services Division, Bay Area Air Quality Management District.

uncertainty. More recently, emissions were shown to depend on driving conditions in a Swedish tunnel that includes both uphill and downhill sections, with emission factors in grams per kilometer increasing by a factor of up to 10 during congested driving periods compared to smooth driving conditions (17).

The goal of the present research is to measure on-road vehicle emissions of CO, CO₂, NO_x, and NMHC as functions of both vehicle speed and specific power. These parameters were chosen as the closest observable on-road analogues to engine speed and mean effective pressure used in engine dynamometer studies to define operating conditions. Specific power (SP) is the power required at the tire–roadway interface divided by vehicle mass. SP is closely related to road load (23) and total tractive power (8). Jimenez-Palacios (6) has shown that CO, VOC, and NO_x emissions are better correlated with SP than with other common single parameters such as speed, acceleration, or power. In this work, we report high-time resolution measurements of CO, CO₂, and NO_x emissions inside a highway tunnel. In most other tunnel studies, only 1-h average or longer integrated results are reported, which greatly reduces the ability to capture effects of changes in driving conditions on emissions.

Experimental Section

Field Measurement Site. Vehicle emissions were measured in a highway tunnel in northern California. The Caldecott Tunnel is located on Highway 24 in the San Francisco Bay area and connects the inland communities of Contra Costa County with Oakland, Berkeley, and San Francisco. The tunnel has three bores, each with two lanes of traffic. The center bore of the tunnel is 970 m long on a 4.1% grade. Heavy-duty vehicles are restricted from the center bore of the tunnel, allowing measurements of light-duty vehicle emissions in this bore. The center bore is not directly accessible from nearby on-ramps, so vehicles are expected to be operating in a warmed-up mode. The direction of vehicles driving through the center bore is changed to accommodate the dominant traffic direction, so emissions due to both low-load conditions (downhill and westbound) and higher-load conditions (uphill and eastbound) can be measured at one site. Traffic volume varies over the course of the day, which also affects vehicle speed and engine load inside the tunnel.

Sampling Schedule. Vehicle emissions were measured on weekdays in July and August 2001. Downhill driving conditions were studied on five mornings from 5 to 11 a.m. Emissions from vehicles traveling uphill in the afternoon and evening were measured over 9 sampling days. Fridays were not included in the uphill driving analysis because afternoon traffic volume peaks earlier in the afternoon, changing driving conditions in the tunnel, and fleet composition on Friday afternoons differs from the rest of the work week. In most cases, afternoon sampling took place from 2 to 8 p.m., but sampling was extended to 10 p.m. on some days to capture emissions occurring under higher-speed driving conditions.

Pollutant Measurements. Continuous measurements of CO, CO₂, and NO_x were made at both the west and east ends of the center bore of the tunnel. CO and CO₂ were measured using gas–filter correlation spectrometers (Thermo Environmental Instruments models 48 and 41H, respectively). NO_x concentrations were measured using TEI model 42 chemiluminescent analyzers. Analyzers were housed in temperature-controlled chambers in order to minimize the effect of changes in ambient temperature on the measurements. Sampling at the west end of the tunnel took place through a window about 4 m above the roadway surface and 12 m from the west limit of the tunnel structure. Sampling at the east end of the tunnel occurred through a ventilation

opening in the ceiling of the traffic bore about 6 m above the roadway and 43 m from the east limit of the tunnel structure. Residence time of gases in the Teflon sampling lines was kept below 15 s at both ends of the tunnel. Pollutant concentrations were recorded as 5-min average values on data loggers.

Calibration checks of the gas analyzers were performed every other day using $\pm 1\%$ NIST traceable gas mixtures. In addition, the Bay Area Air Quality Management District performed audits on the CO, CO₂, and NO_x analyzers at both ends of the tunnel at the beginning and end of this study. The average deviation of readings from audit values was within -3 to $+1\%$ for CO and CO₂ analyzers and within -5 to $+1\%$ for NO_x analyzers in all four audits. In addition, the California Air Resources Board audited the CO and NO_x analyzers at the east end of the tunnel in the middle of the field study. The average difference between the analyzer readings and audit values was $+1.1\%$ for CO and -3.9% for NO_x. We did not make any adjustments to raw data measured at the tunnel based on results of these audits.

Integrated air samples were collected at both ends of the tunnel at the same measurement locations as for other pollutants. Air samples were collected in stainless steel canisters during high-traffic periods for both downhill (6–8 a.m.) and uphill (4–6 p.m.) driving. Samples were analyzed by the Bay Area Air Quality Management District to quantify speciated non-methane hydrocarbons plus MTBE concentrations (for convenience, referred to here collectively as NMHC) using gas chromatography with flame ionization detection. Details regarding the chromatographic columns and temperature programs have been presented previously by Kirchstetter et al. (24). Canister sampling periods were chosen to maximize the chance of observing the same vehicles traveling through the center bore, westbound in the morning and eastbound in the afternoon.

Tunnel Ventilation. During this study, ventilation fans at both ends of the tunnel were turned off, so there was only longitudinal air flow due primarily to the flow of traffic. Determination of fuel consumption by the vehicle fleet driving through the tunnel requires knowledge of this air flow rate. Sulfur hexafluoride (SF₆) tracer gas was released at a constant rate of 1.16 g min^{-1} at the tunnel entrance, and its concentration was measured continuously at the tunnel exit. A four-point SF₆ injection system powered by a fan promoted mixing of tracer gas with tunnel air. An on-line gas chromatograph (Hewlett-Packard model 5890) with electron capture detector was used to measure SF₆ concentrations at the other end of the tunnel, allowing for determination of tunnel air flow rate every 5 min.

Traffic Monitoring. Average vehicle speed inside the tunnel was determined using video cameras with synchronized clocks that were situated at both ends of the tunnel. Transit times measured for individual vehicles were combined with known tunnel length to calculate vehicle speeds. Vehicle transit times were determined from the videotapes every 3 min. It was found that measuring the speed of one or two vehicles for each 5-min measurement period was representative of vehicle speeds for the entire 5-min period. When stalls or accidents occurred in the tunnel, traffic flow was disrupted for up to 20 min. This occurred on three occasions during the field study in the afternoon sampling periods.

A radar gun was moved from one end of the tunnel to the other to measure vehicle speeds entering and exiting the tunnel. If entrance and exits speeds differ from each other and from average speeds, this indicates acceleration or deceleration inside the tunnel. Except during the morning and afternoon commuter peak periods, vehicle entrance, exit, and average speeds inside the tunnel were all the same, within the uncertainties of these measurements. During both

morning and afternoon rush hour, traffic congestion occurs upstream of the tunnel, so vehicles accelerate gradually inside the tunnel. Average acceleration in the tunnel was estimated using measured tunnel entrance and exit speeds combined with findings of a prior instrumented vehicle study that logged speed as a function of position inside the tunnel (19).

Counts were made of the numbers of vehicles traveling through the tunnel for four separate categories: cars, light-duty trucks, motorcycles, and medium/heavy-duty vehicles. Light-duty trucks include pickups, sport-utility vehicles, vans, and minivans; medium/heavy-duty vehicles include buses, trucks with 2 axles and 6 tires (medium), and trucks with 3 or more axles (heavy). Traffic was counted over 5-min periods once every 15 min during this study. A video camera was used to record license plates of light-duty vehicles driving through the tunnel on a weekday afternoon/evening sampling period and on a separate weekday morning. From this videotape, the license plates of at least 250 vehicles passing through the tunnel each hour were recorded and matched to vehicle registration data from the California Department of Motor Vehicles.

Results and Discussion

Emission Factors for CO and NO_x. Increases in CO₂, CO, and NO_x concentrations between tunnel entrance and exit varied depending on pollutant, traffic direction, and traffic volume. For downhill driving, typical increases in concentration were 100–150 ppm for CO₂, 2–3 ppm for CO, and 90–130 ppb for NO_x. For uphill driving where more fuel is being burned, concentrations from entrance to exit typically increased by 200–600 ppm for CO₂, 10–15 ppm for CO, and 400–1100 ppb for NO_x. Average emissions of vehicles traveling through the tunnel were determined by carbon balance using known gasoline properties. Fleet-averaged emission factors (E_p) are expressed per liter of fuel burned:

$$E_p = \left(\frac{\Delta[P]}{\Delta[\text{CO}_2] + \Delta[\text{CO}]} \right) \left(\frac{MW_p}{MW_C} \right) w_C \rho_f \quad (1)$$

In eq 1, $\Delta[P]$ is the increase in concentration of pollutant P measured between tunnel entrance and exit, MW_p is the molecular weight of pollutant P (g mol^{-1}), $MW_C = 12 \text{ g mol}^{-1}$, $w_C = 0.85$ is the weight fraction of carbon in oxygenated gasoline, and gasoline density $\rho_f = 740 \text{ g L}^{-1}$. Organic compounds have been ignored in the denominator of eq 1; the hydrocarbon contribution to total carbon concentrations in the tunnel is negligible as compared to CO₂ and CO. Emission factors for CO and NO_x were calculated over 5-min averaging periods. Trends in light-duty vehicle emissions measured at this tunnel site during the period 1994–2001 are presented elsewhere (25).

Figure 1 presents average emission factors for CO with associated 95% confidence intervals as a function of time of day. For downhill driving conditions during morning hours, average CO emission factors were between 16 and 34 g L^{-1} , with greater variability at a given time of day as compared to uphill measurements. Variability results in part from a lower signal-to-noise ratio for downhill driving. Also note that downhill emissions were sampled on 5 d as compared to 9 d for uphill driving. Uphill driving conditions observed during afternoon and evening hours had average CO emission factors between 27 and 75 g L^{-1} with low emission factors between 4:00 and 6:30 p.m. and higher emission factors both before and after this peak traffic period. While the CO emission factor (normalized to fuel consumption) for downhill driving was not significantly different from the uphill measurements from 4 to 6:30 p.m., CO emission factors during off-peak hours in the early afternoon and evening increased by a factor of 2.

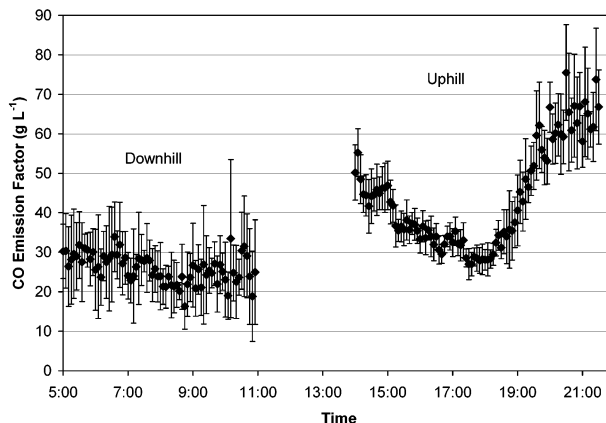


FIGURE 1. CO emission factor ($\pm 95\%$ CI) as a function of time of day (PDT).

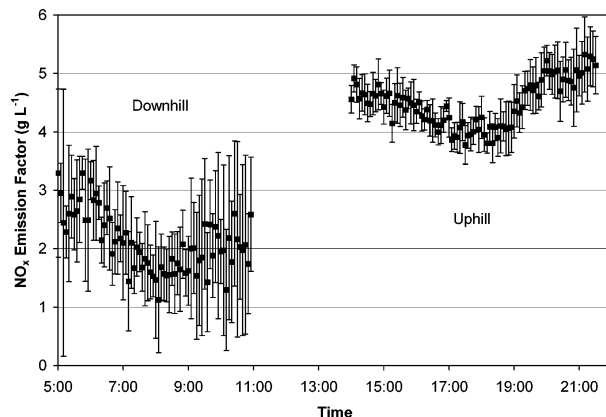


FIGURE 2. NO_x emission factor ($\pm 95\%$ CI) as a function of time of day.

NO_x emission factors (as NO₂) are shown in Figure 2. Average emission factors for downhill driving in the morning ranged from 1.1 to 3.3 g L^{-1} . A trend of decreasing NO_x emission factors over the first half of the morning may be present. For uphill driving, NO_x emission factors typically ranged between 3.8 and 5.3 g L^{-1} . NO_x emissions for downhill driving were lower than for uphill driving during the 4–6:30 p.m. peak period. In the afternoon, NO_x emission factors were high before rush hour, reached a minimum during the 4–6:30 p.m. period, and were at a maximum at the end of the day. While both CO and NO_x emission factors showed this pattern, CO emission factors varied more than NO_x over the course of the afternoon and evening.

Traffic Characterization. Figure 3 and Table 1 show that average traffic volume ranged from 1700 to 4400 vehicles per hour in the center bore of the tunnel. In addition to changes in traffic volume and vehicle speeds during the day, another factor that may contribute to changes in emission factors is the composition of the vehicle fleet. For example, the light-duty (LD) truck fraction varied between 30 and 50% with time of day, as shown in Figure 3. For downhill driving, the fraction of LD trucks was at a minimum during the morning rush hour. The fraction of LD trucks in the early afternoon was $\sim 50\%$ and gradually decreased to 30% over the course of the afternoon and evening. In contrast, Figures 1 and 2 indicate that CO and NO_x emission factors increased after 6 p.m., while the LD truck fraction continued to decrease. Although LD trucks are required to meet less stringent exhaust emission standards than cars on a gram per kilometer basis, these trucks also have higher fuel consumption than cars. When expressed per unit of fuel burned, exhaust emission standards for new cars and LD trucks are similar (26, 27).

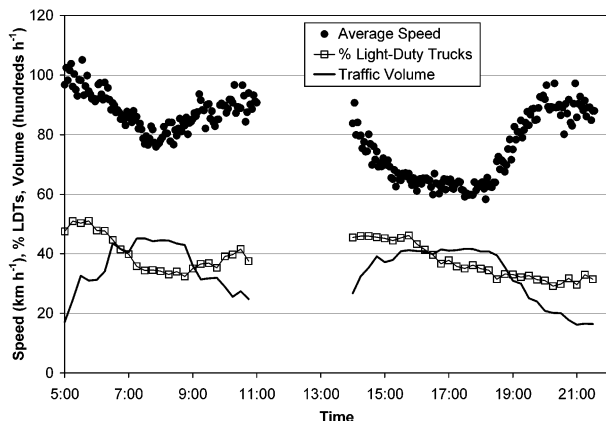


FIGURE 3. Average vehicle speed, percentage of light-duty trucks in the fleet, and total traffic volume as a function of time of day.

TABLE 1. Hourly Average (± 1 SD) Fleet Characteristics and Ambient Temperature

time ^a (PDT)	speed (km h ⁻¹)	traffic vol ^b	% light- duty trucks ^c	model year ^d	temp (°C)
05:00	97 \pm 7	2590 \pm 630	50 \pm 3	1995.3 \pm 5.3	12 \pm 2
06:00	90 \pm 7	3720 \pm 590	46 \pm 4	1995.1 \pm 5.5	12 \pm 3
07:00	81 \pm 6	4370 \pm 300	36 \pm 3	1995.8 \pm 5.0	12 \pm 3
08:00	82 \pm 6	4360 \pm 280	33 \pm 2	1995.7 \pm 5.1	13 \pm 3
09:00	88 \pm 6	3290 \pm 220	36 \pm 3	1995.7 \pm 4.6	14 \pm 3
10:00	91 \pm 7	2640 \pm 300	39 \pm 3	1996.1 \pm 5.1	15 \pm 3
14:00	76 \pm 9	3340 \pm 510	46 \pm 3	1995.4 \pm 5.4	18 \pm 3
15:00	64 \pm 13	3930 \pm 510	45 \pm 3	1994.7 \pm 6.1	18 \pm 2
16:00	64 \pm 6	4080 \pm 180	40 \pm 4	1995.4 \pm 4.9	18 \pm 2
17:00	62 \pm 5	4140 \pm 140	36 \pm 3	1995.8 \pm 5.0	17 \pm 2
18:00	67 \pm 11	3910 \pm 360	34 \pm 3	1994.6 \pm 5.6	17 \pm 3
19:00	84 \pm 11	2750 \pm 390	32 \pm 3	1994.7 \pm 5.6	16 \pm 3
20:00	90 \pm 7	1970 \pm 200	30 \pm 1	1995.4 \pm 5.1	14 \pm 2
21:00	89 \pm 4	1690 \pm 250	31 \pm 2	1996.0 \pm 5.0	14 \pm 2

^a Time at the beginning of each 1-h averaging period. ^b Number of vehicles per hour. ^c The rest of the vehicles observed in the tunnel were almost all cars. The average motorcycle fraction was <1%, medium-duty trucks were <0.3%, and heavy-duty vehicles were <0.1% of total traffic. ^d Average model year of the light-duty vehicle fleet.

The fraction of medium-duty trucks in the tunnel fleet varied between 0 and 0.3%, and heavy-duty truck traffic typically accounted for 0.05% of the fleet; these fractions are too low to affect the present measurements of light-duty vehicles significantly.

The age distribution is another characteristic of the vehicle fleet that may influence emission factors measured at the tunnel, other factors being equal. A newer vehicle fleet would be expected to have lower pollutant emissions. The average model year of vehicles inside the tunnel gradually increased (i.e., more newer vehicles) over the morning, ranging from 1995.1 to 1996.1. As an indication of random variation in the vehicle fleet age, comparison of consecutive 5-min periods of traffic commonly returned differences of half a model year. Over the course of the day, all the observed age distributions were similar. The average age of the fleet during the afternoon uphill driving period ranged from 1994.7 to 1996.0 with no clear trend over the afternoon. Both the 4–6 p.m. and the 8–10 p.m. periods had newer vehicle fleets than other p.m. time periods. Note in Figures 1 and 2 that the lowest emission factors for uphill driving occurred during 4–6 p.m. and the highest occurred after 8 p.m. Although changes in the average age of vehicles would be expected to affect emissions, changes in vehicle age observed at the tunnel over the time scale of hours do not explain the emissions trends shown in Figures 1 and 2, especially the large increase in CO and NO_x emission factors in the evening when newer vehicles were present in largest proportion.

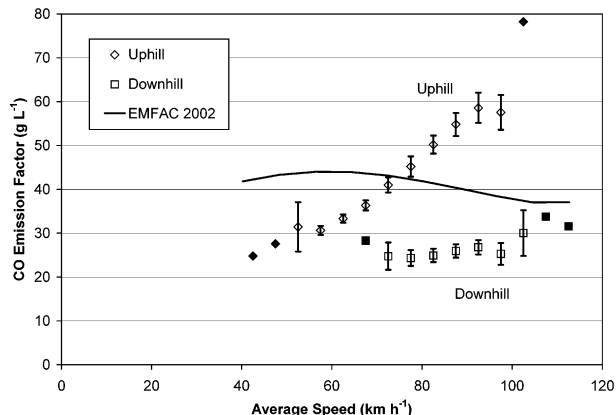


FIGURE 4. CO emission factor ($\pm 95\%$ CI) vs average vehicle speed with comparison to EMFAC2002. Data are organized into 5 km h⁻¹ bins and plotted vs the speed bin average. Closed symbols represent speed bins with single data points.

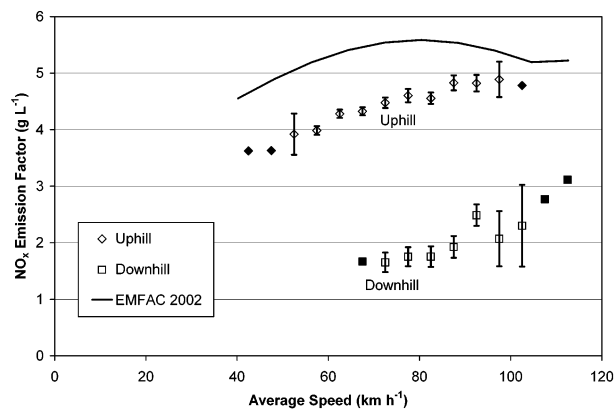


FIGURE 5. NO_x emission factor ($\pm 95\%$ CI) vs average vehicle speed with comparison to EMFAC2002. Data are organized into 5 km h⁻¹ bins and plotted vs the speed bin average. Closed symbols represent speed bins with single data points.

Emission Factor Dependence on Vehicle Speed. Motor vehicle emissions are known to depend on engine load, with distance-based emission factors showing greater variability than fuel-based factors (16). The change in engine load from downhill to uphill driving will contribute to differences between morning and afternoon emission factors. Additional engine load effects may be caused by changes in vehicle speed shown in Figure 3. For downhill driving, speeds were typically 80–100 km h⁻¹, with a minimum occurring between 7 and 9 a.m. when traffic volume was highest. For uphill driving in the afternoon, average speeds were typically 60–90 km h⁻¹. Minimum vehicle speeds occurred when traffic volume was greatest, from 4:00 to 6:30 p.m. During this period gradual acceleration occurs inside the tunnel, whereas at off-peak hours vehicles enter and exit the tunnel at the same speed.

In comparing vehicle speeds shown in Figure 3 with CO and NO_x emissions shown in Figures 1 and 2, a correlation is apparent, particularly in the afternoon. To show the relationship more clearly, Figures 4 and 5 present emissions behavior as a function of average driving speed of the fleet through the tunnel. As shown in Figure 4, the CO emission factor depends strongly on speed for uphill driving and is independent of speed for downhill driving. The NO_x emission factor (Figure 5) also varies with vehicle speed for uphill driving, although less strongly than CO emissions.

Also included in Figures 4 and 5 are comparisons to predictions of the California Air Resources Board EMFAC emission factor model (28). Representative average values of

air temperature, relative humidity, and light-duty truck fraction were assumed in these comparisons. Direct comparison of tunnel results with EMFAC should be made with caution because the tunnel data shown in these figures are for driving on a ~4% grade, whereas EMFAC predictions are for driving on level terrain. Furthermore EMFAC predictions for a given average speed implicitly involve a range of driving conditions, whereas the tunnel measurements are usually for a much narrower range of driving conditions. For instance, EMFAC predictions for an average speed of 80 km h⁻¹ represents emissions over a driving cycle with a maximum speed of 122 km h⁻¹ and a small amount of time at idle. It should be noted that EMFAC is not designed to predict emissions behavior at speeds above 105 km h⁻¹; emission factors that are the same as for 105 km h⁻¹ are output when higher speeds are specified in the model input. In Figure 4, the fuel-based CO emission factors predicted by EMFAC are similar to tunnel measurements when normalized to fuel consumption. Variations in EMFAC-derived predictions of CO emissions with vehicle speed are minor. This is consistent with tunnel results for downhill but not uphill driving. In Figure 5, EMFAC predictions for NO_x are similar to tunnel measurements for uphill driving; NO_x emissions are lower for downhill driving.

Emission Factor Dependence on Specific Power. CO and NO_x emission factors are presented here as a function of a single engine load parameter: SP. SP is the sum of external forces opposing vehicle motion multiplied by vehicle speed and divided by vehicle mass. In the same way that mean effective pressure is more useful than torque when discussing engines of varying size, SP is more useful than power when comparing vehicles of different size because engine power typically scales with vehicle mass. Average specific power for each 5-min sampling period is calculated as follows:

$$SP = \left[\frac{C_D A_f \rho_a}{m} (v + v_w)^2 + g C_R + a(1 + \epsilon_i) + g \sin \theta \right] v \quad (2)$$

where C_D is the drag coefficient, A_f is the vehicle frontal area, ρ_a is the density of air, v is the average vehicle speed, a is the estimated average vehicle acceleration for the 5-min period in question, v_w is the headwind speed (negative here because air flow inside the tunnel is in the same direction as the traffic), g is the acceleration due to gravity, C_R is the coefficient of rolling resistance of the tires, ϵ_i is the equivalent translational mass of rotating components of the drivetrain, and $\theta = \tan^{-1}(\text{grade})$ is the angle of the roadway with the horizontal. When dividing the resistive forces by vehicle mass, note in eq 2 that m cancels in three of the four external forces: rolling resistance, acceleration, and grade. As the vehicle mass remains in only one term, the calculation of SP is not highly dependent on vehicle mass. Values of $C_D A_f m^{-1}$ lie between 0.0004 and 0.0007 for most light-duty vehicles in the United States (29), and a typical value of 0.0005 has been recommended (6). Drag coefficients for large vehicles can be influenced by proximity to tunnel walls, but this effect is not important for light-duty vehicles (30). Values for C_R range from 0.0085 to 0.016, with 0.0135 recommended as a typical value (6). ϵ_i is gear-dependent and ranges between 0.075 and 0.25, with 0.1 recommended for calculations of SP (6). Because of engine and transmission friction, SP values slightly below zero still require a small amount of engine power when vehicles are in gear. Use of typical values when calculating SP is appropriate here because we are estimating the average SP of a fleet of vehicles. SP does not include estimates of engine accessory loads, notably that due to use of air conditioning. It is difficult to quantify here how many vehicles were using air conditioning. Note however that over the course of the present study, mild temperature conditions prevailed: the minimum and maximum observed air tem-

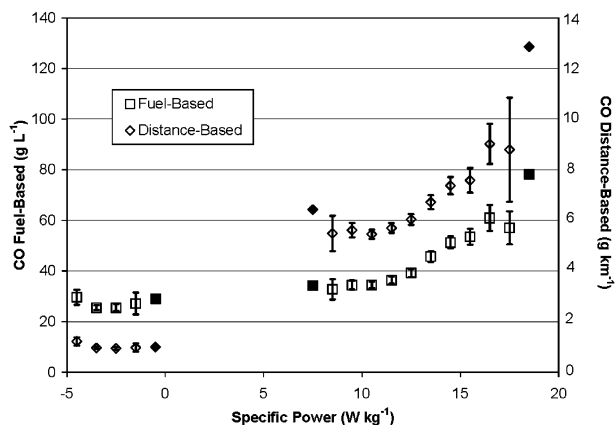


FIGURE 6. CO emission factors plotted versus specific power. Data are organized into 1 W kg⁻¹ bins and plotted vs the SP bin average. Closed symbols represent SP bins with single data points.

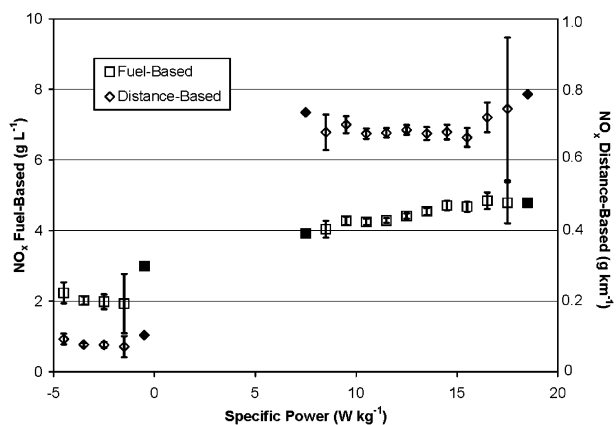


FIGURE 7. NO_x emission factors plotted vs specific power. Data are organized into 1 W kg⁻¹ bins and plotted vs the SP bin average. Closed symbols represent SP bins with single data points.

perature at a nearby meteorological tower were 10 and 24 °C (see Table 1 for hourly average values throughout the day). Mild prevailing temperatures suggest that extensive use of vehicle air conditioning systems did not occur during this study.

Downhill driving at the Caldecott Tunnel resulted in average SP values between -5 and 0 W kg⁻¹. Uphill driving resulted in SP between 7 and 18 W kg⁻¹, with lower SP values observed during rush hour, and the highest SP occurring at night when vehicle speeds were also highest. For comparison, a typical vehicle cruising on a level road at $v = 105$ km h⁻¹ has $SP = 11$ W kg⁻¹. As shown in Figure 6, fuel-based CO emission factors are independent of load below 11 W kg⁻¹, with increasing CO emission factors observed above $SP = 11$ W kg⁻¹. Driving in the Caldecott Tunnel does not typically exceed the maximum SP of 25 W kg⁻¹ encountered during the city driving portion of the Federal Test Procedure emissions certification test. Previous studies have reported increases in CO emissions due to increasing load but only at engine loads greater than those encountered during certification testing (3, 5, 6, 9). NO_x emissions are shown as a function of SP in Figure 7. For uphill driving conditions, NO_x emissions also increase with load, although the rate of increase is less than for CO emissions (compare Figures 6 and 7). In contrast to the dependence of fuel-normalized NO_x emissions on engine load noted here, Pierson et al. (16) reported nearly identical NO_x emission factors for downhill and uphill driving in the Fort McHenry Tunnel.

Our methodology for calculating average SP is best suited for estimating engine load during nonpeak hours when

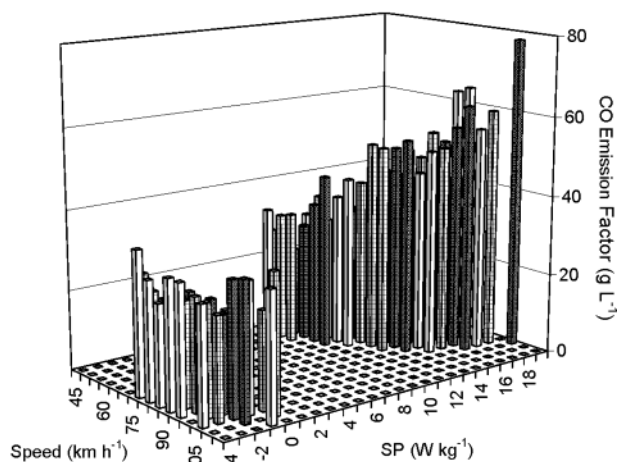


FIGURE 8. CO emission factor as a function of both average vehicle speed (5 km h⁻¹ bins) and specific power (1 W kg⁻¹ bins). The bin labels shown correspond to the bin maxima, except for the zero bin, which has negligible width.

driving through the tunnel was steady state and emission factors for CO and NO_x were elevated. Accelerations that occur during rush hour may have a nonlinear affect on emissions, but we calculate SP based on average acceleration. Emissions are low during periods when acceleration is occurring in the tunnel, suggesting that these nonlinearities do not play an important role here.

Emissions of CO and NO_x have been shown to increase with both speed and SP, but the question remains whether a combination of both variables is better able to describe on-road vehicle emissions than either one alone. Figure 8 presents the CO emission factor as a function of both speed and SP. Note the number of data points that are included in each bin differs depending on how frequently those driving conditions were observed at the tunnel. Inspection of the data for positive SP shows that, for a given value of SP, emissions are a function of vehicle speed. Therefore, exhaust emissions are functions of both vehicle speed and SP—neither parameter alone captures all of the relevant effects. The same conclusion applies to the NO_x emission factor (not shown), but variations in the NO_x emission factor over all observed uphill driving conditions were less than those observed for CO.

NMHC Emissions. Although high time resolution measurements of NMHC were not made in this study, it is possible to compare NMHC emissions for downhill versus uphill driving using results of 2-h integrated air samples (collected 6–8 a.m. and 4–6 p.m., respectively). To provide context for these measurements, traffic volume through the tunnel bore was ~4100 vehicles per hour and average model year was ~1995.5 during all NMHC sampling periods. The average light-duty truck fraction in the fleet was 41 ± 6% (morning samples/downhill driving) and 38 ± 4% (afternoon samples/uphill driving). Vehicle speeds were higher for downhill driving (86 versus 63 km h⁻¹), resulting in average SP values of -4 W kg⁻¹ during downhill driving and +11 W kg⁻¹ for uphill driving during peak traffic periods.

During downhill driving from 6 to 8 a.m., the average increase in NMHC concentration going from tunnel entrance to exit was 480 μg m⁻³ as compared to 670 μg m⁻³ for uphill driving from 4 to 6 p.m. The NMHC emission factor for downhill driving was 4.3 ± 0.5 g L⁻¹ as compared to 1.3 ± 0.1 g L⁻¹ for uphill driving. When normalized to fuel consumption, the emission factor for low-load driving is over 3 times greater than the NMHC emission factor for uphill driving. In contrast, a study performed in the Fort McHenry Tunnel in Baltimore in 1992 showed similar NMHC emission

factors for uphill and downhill driving (16). The EMFAC model predicts emissions of reactive organic gases to be 1.6–2.0 g L⁻¹ for the range of vehicle speeds observed at the tunnel; note again it was not possible to account for roadway grade effects within EMFAC. The reason for higher NMHC emission factors during downhill as compared to uphill driving is not clear, though this effect has been observed before (7) and may be due to enleanment of the fuel/air ratio which occurs during load reduction events and during long deceleration (31). While the emission rates differed, the composition of NMHC emissions for uphill and downhill driving was almost indistinguishable. The fraction of unburned fuel in tunnel NMHC emissions was 79 ± 2% for uphill driving as compared to 84 ± 1% during downhill driving. Differences in composition include: ethene, propene, and benzene which were 20–50% more abundant for uphill driving, and 2-methylpentane, 2,2,4-trimethylpentane, and methylcyclopentane, which were 20–35% more abundant in downhill emissions.

Fuel Consumption. Fleet-average fuel consumption (FC) in liters per 100 vehicle-km traveled was calculated using the following equation:

$$FC = \frac{E_{SF_6}}{[SF_6]} \frac{[\Delta C]}{\rho_f w_C N \frac{L}{100}} \quad (3)$$

where $E_{SF_6} = 1.16 \times 10^6 \mu\text{g min}^{-1}$ is the SF₆ injection rate at the tunnel entrance, [SF₆] is the measured SF₆ concentration at tunnel exit (μg m⁻³), [ΔC] is the change in total carbon concentration from tunnel entrance to exit (μg C m⁻³, mainly from CO₂), $\rho_f = 740 \times 10^6 \mu\text{g L}^{-1}$ is gasoline density, $w_C = 0.85$ is the weight fraction of carbon in gasoline, N is the observed traffic volume (vehicles min⁻¹), and $L = 0.91$ km is the tunnel length between sampling points.

Fuel consumption for downhill driving (3.6 ± 0.1 L/100 km) is 20–25% of the uphill consumption. Fuel consumption for vehicles driving through the tunnel during 4–6:30 p.m. when traffic volume is high was 16.4 ± 0.1 L/100 km as compared to 14.2 ± 0.3 L/100 km during off-peak uphill driving. While engine loads are greater during higher-speed driving through the tunnel, the lack of acceleration during off-peak hours means the fuel energy is being used to cover a given distance more efficiently.

Distance-Based Emission Factors. Emission factors for CO, NO_x, and NMHC expressed per kilometer traveled can be calculated from measured fuel consumption and the fuel-based emission factors presented previously. Figures 6 and 7 include distance-based emission factors for CO and NO_x as a function of SP. Distance-based emission factors for these two pollutants show greater dependence on load than fuel-based emission factors. The CO emission factor for downhill driving was ~1 g km⁻¹ and for uphill driving ranged between 5.5 and 13 g km⁻¹. NO_x emission factors at the tunnel were ~0.08 g km⁻¹ for downhill driving and ranged from 0.65 to 0.80 g km⁻¹ for uphill driving. For both CO and NO_x, an order of magnitude increase in emissions expressed per kilometer traveled was observed for uphill driving as compared to downhill. While this study shows that both fuel-based and distance-based emission factors for CO and NO_x depend on driving conditions, distance-based factors require larger adjustments in emission inventory calculations to account for the effects of variations in driving conditions.

It is surprising that the average increase in NMHC concentration between tunnel entrance and exit was 480 μg m⁻³ for downhill driving as compared to an increase of 670 μg m⁻³ for uphill driving. A smaller increase was expected from tunnel entrance to exit for downhill driving, as observed for other pollutants. Distance-based NMHC emission factors are nearly the same: 0.16 ± 0.02 g km⁻¹ for downhill driving and 0.21 ± 0.02 g km⁻¹ for uphill driving. The finding that

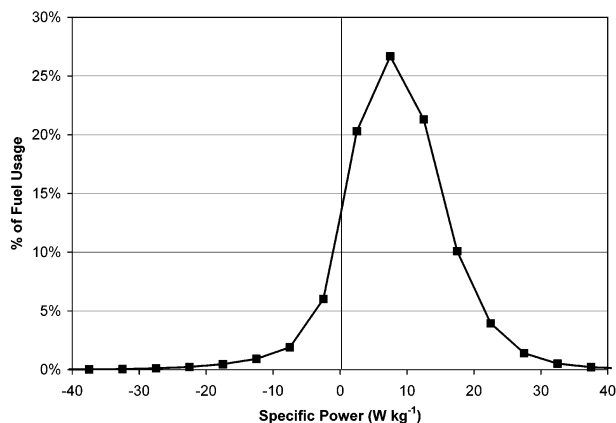


FIGURE 9. Distribution of fuel usage as a function of specific power calculated for the full range of vehicle operating conditions observed in instrumented vehicle studies performed in the early 1990s (32). The bin width is 5 W kg^{-1} . Values are plotted against the bin midpoint. Data outside of the range shown account for $<0.2\%$ of total fuel usage. Idle conditions (not shown) accounted for $\sim 6\%$ of total fuel use.

distance-based emission factors for NMHC vary less with driving conditions than fuel-based emission factors differs from findings reported here for CO and NO_x , and from findings for NMHC reported by Pierson et al. (16).

Emissions measured during times when a stall or accident occurred in the tunnel provide a further opportunity to compare fuel-normalized and distance-normalized emission factors. Sjödin et al. (17) found that distance-based emission factors increased by a factor of up to 10 during congestion as compared to smooth driving conditions. During the present study, there were 11 5-min sampling periods during which traffic flow was disrupted due to stalled vehicles inside the tunnel. The need for traffic to merge into a single lane to get past the stalled vehicle led to severe congestion followed by acceleration back to normal driving speeds. During such events (all were for uphill driving during the afternoon), average speeds ranged from 14 to 27 km h^{-1} inside the tunnel. Fuel-based emission factors were $23\text{--}65 \text{ g L}^{-1}$ for CO and $2.3\text{--}3.8 \text{ g L}^{-1}$ for NO_x . During these same periods, distance-based emission factors were $6\text{--}18 \text{ g km}^{-1}$ for CO and $0.4\text{--}1.1 \text{ g km}^{-1}$ for NO_x ; the increase in emissions due to traffic congestion was less than that observed by Sjödin et al. (17). While fuel-based emission factors measured when stalled vehicles blocked traffic are similar to those observed at other times, the distance-based values measured during these abnormal events are at the upper end of the range observed during the rest of the study. Again, fuel-based emission factors for CO and NO_x are less sensitive to disruptions in normal driving patterns than emission factors expressed per kilometer traveled.

Comparison to Typical Driving Conditions. Emission factors as functions of vehicle speed and SP have been presented for various driving conditions. Here we compare the range of driving conditions observed at the tunnel with instrumented vehicle studies conducted in the early 1990s that characterize the full distribution of vehicle operating conditions (32). Despite being 10 yr old, these data are the best available as more recent large-scale studies of vehicle operating conditions in the United States have not been reported. About 100 privately owned passenger vehicles in each of three urban areas were instrumented with data loggers. The data loggers recorded vehicle speed, engine speed, and intake manifold vacuum (an indication of throttle position) at 1 Hz whenever the engine was operating. Acceleration can be calculated from changes in vehicle speed over 1-s intervals. Instantaneous fuel consumption for this

group of vehicles was estimated using a model proposed by Ross and co-workers (31, 33, 34), which relates fuel energy input to brake power output and losses within the engine. The calculated distribution of fuel usage as a function of specific power is presented in Figure 9. The range of driving conditions observed during the present tunnel investigation encompasses a large portion of fuel usage. By interpolation of results shown in Figures 6 and 7, emission factors for conditions that account for $\sim 75\%$ of fuel usage can be estimated. Driving conditions that are not well-represented inside the tunnel include idling, stop-and-go driving, high-speed ($> 100 \text{ km h}^{-1}$), and high-load ($> 20 \text{ W kg}^{-1}$) conditions, which together account for the remaining $\sim 25\%$ of total fuel usage.

Acknowledgments

The authors thank Robert Franicevich, James Hesson, and Daniel Zucker of the Bay Area Air Quality Management District; Bryce Wilson of UC Berkeley; David Littlejohn and Douglas Sullivan of Lawrence Berkeley National Laboratory; Gregory Sweet of the California Bureau of Automotive Repair; and the Caltrans staff at the Caldecott Tunnel. Financial support was provided by the University of California Transportation Center with major in-kind support from the Technical Services Division of the Bay Area Air Quality Management District.

Literature Cited

- (1) *National Air Quality and Emission Trends Report, 1999*, EPA-454/R-01-004; U.S. Environmental Protection Agency, Office of Air Quality: Research Triangle Park, NC, 2001.
- (2) Kelly, N. A.; Groblicki, P. J. *J. Air Waste Manage. Assoc.* **1993**, *43*, 1351–1357.
- (3) Haskew, H. M.; Cullen, K.; Liberty, T. F.; Langhorst, W. K. *SAE Tech. Pap. Ser.* **1994**, No. 94C016.
- (4) St. Denis, M. J.; Cicero-Fernandez, P.; Winer, A. M.; Butler, J. W.; Jesion, G. *J. Air Waste Manage. Assoc.* **1994**, *44*, 31–38.
- (5) Cicero-Fernandez, P.; Long, J. R.; Winer, A. M. *J. Air Waste Manage. Assoc.* **1997**, *47*, 898–904.
- (6) Jimenez-Palacios, J. L. Ph.D. Dissertation, Massachusetts Institute of Technology, 1999; pp 54–103.
- (7) Zhang, Y.; Stedman, D. H.; Bishop, G. A.; Guenther, P. L.; Beaton, S. P.; Peterson, J. E. *Environ. Sci. Technol.* **1993**, *27*, 1885–1891.
- (8) Barth, M.; An, F.; Norbeck, J.; Ross, M. *Transp. Res. Rec.* **1996**, *1520*, 81–88.
- (9) An, F.; Ross, M. *J. Air Waste Manage. Assoc.* **1996**, *46*, 216–223.
- (10) Washington, S.; Leonard, J. D.; Roberts, C. A.; Young, T.; Sperling, D.; Botha, J. *Int. J. Vehicle Des.* **1998**, *20*, 351–359.
- (11) Fomunung, I.; Washington, S.; Guensler, R. *Transp. Res. Part D* **1999**, *4*, 333–352.
- (12) Sturm, P. J.; Kirchweyer, G.; Hausberger, S.; Almbauer, R. A. *Int. J. Vehicle Des.* **1998**, *20*, 181–191.
- (13) Knepper, J. C.; Koehl, W. J.; Benson, J. D.; Burns, V. R.; Gorse, R. A., Jr.; Hochhauser, A. M.; Leppard, W. R.; Rapp, L. A.; Reuter, R. M. *SAE Tech. Pap. Ser.* **1993**, No. 930137.
- (14) *Modeling Mobile Source Emissions*, Transportation Research Board, National Research Council: Washington, DC, 2000; pp 135–166.
- (15) Staehelin, J.; Schlapfer, K.; Burgin, T.; Steinemann, U.; Schneider, S.; Brunner, D.; Baumle, M.; Meier, M.; Zahner, C.; Keiser, S.; Stahel, W.; Keller, C. *Sci. Total Environ.* **1995**, *169*, 141–147.
- (16) Pierson, W. R.; Gertler, A. W.; Robinson, N. F.; Sagebiel, J. C.; Zielinska, B.; Bishop, A. W.; Stedman, D. H.; Zweidinger, R. B.; Ray, W. D. *Atmos. Environ.* **1996**, *30*, 2233–2256.
- (17) Sjödin, A.; Persson, K.; Andreasson, K.; Arlander, B.; Galle, B. *Int. J. Vehicle Des.* **1998**, *20*, 147–158.
- (18) Rogak, S. N.; Pott, U.; Dann, T.; Wang, D. *J. Air Waste Manage. Assoc.* **1998**, *48*, 604–615.
- (19) Kirchstetter, T. W.; Singer, B. C.; Harley, R. A.; Kendall, G. R.; Traverse, M. *Environ. Sci. Technol.* **1999**, *33*, 318–328.
- (20) Touaty, M.; Bonsang, B. *Atmos. Environ.* **2000**, *34*, 985–996.
- (21) Schmid, H.; Pucher, E.; Ellinger, R.; Biebl, P.; Puxbaum, H. *Atmos. Environ.* **2001**, *35*, 3585–3593.
- (22) Hwa, M. Y.; Hsieh, C. C.; Wu, T. C.; Chang, L. F. W. *Atmos. Environ.* **2002**, 1993–2002.
- (23) Heywood, J. B. *Internal Combustion Engine Fundamentals*; McGraw-Hill: New York, 1988.

- (24) Kirchstetter, T. W.; Singer, B. C.; Harley, R. A.; Kendall, G. R.; Hesson, J. M. *Environ. Sci. Technol.* **1999**, *33*, 329–336.
- (25) Kean, A. J.; Sawyer, R. F.; Harley, R. A. *SAE Tech. Pap. Ser.* **2002**, No. 2002-01-1713.
- (26) *Federal and California Exhaust and Evaporative Emission Standards for Light-Duty Vehicles and Light-Duty Trucks*; EPA-420-B-00-001; U.S. Environmental Protection Agency, Office of Air and Radiation: Washington, DC, 2001.
- (27) *Light-Duty Automotive Technology and Fuel Economy Trends: 1975–2001*; EPA-420-R-01-008; U.S. Environmental Protection Agency, Office of Air and Radiation: Washington, DC, 2001.
- (28) *EMFAC2002, V2.2*; California Air Resources Board: Sacramento, CA, 2002.
- (29) Emmelman, H. J.; Hucho, W. H. *Aerodynamics of Road Vehicles*, 4th ed.; Society of Automotive Engineers: Warrendale, PA, 1998.
- (30) John, C.; Friedrich, R.; Staehelin, J.; Schlapfer, K.; Stahel, W. A. *Atmos. Environ.* **1999**, *33*, 3367–3376.
- (31) An, F.; Barth, M.; Scora, G.; Ross, M. *Transp. Res. Rec.* **1998**, *1641*, 48–57.
- (32) *Federal Test Procedure Review Project: Preliminary Technical Report*; U.S. Environmental Protection Agency, Office of Air and Radiation: Washington, DC, 1993.
- (33) An, F.; Ross, M. *SAE Tech. Pap. Ser.* **1993**, No. 930328.
- (34) Ross, M. *Annu. Rev. Energy Environ.* **1994**, *19*, 75–112.

Received for review November 22, 2002. Revised manuscript received April 1, 2003. Accepted June 5, 2003.

ES0263588